Biophysical Chemistry 25 (1986) 223–241
Elsevier

BPC 01106

INTERACTION OF HUMAN LOW DENSITY LIPOPROTEIN AND APOLIPOPROTEIN B WITH TERNARY LIPID MICROEMULSION

PHYSICAL AND FUNCTIONAL PROPERTIES

Paul W. CHUN *, Erich E. BRUMBAUGH ** and Rachel B. SHIREMANN ***

Department of Biochemistry and Molecular Biology, College of Medicine, University of Florida, Gainesville, FL 32610, U.S.A.

Received 28th July 1986
Revised manuscript received 4th September 1986
Accepted 25th September 1986

Key words: Scanning molecular sieve chromatography; LDL-apolipoprotein B–microemulsion interaction

Based on data from sedimentation velocity experiments, electrophoresis, electron microscopy, cellular uptake studies, scanning molecular sieve chromatography using a quasi-three-dimensional data display and flow performance liquid chromatography (FPLC), models for the interaction of human serum low density lipoprotein (LDL) and of apolipoprotein B (apo B) with a ternary lipid microemulsion (ME) are proposed. The initial step in the interaction of LDL (Stokes radius 110 Å) with the ternary microemulsion (Stokes radius 270 Å) appears to be attachment of the LDL to emulsion particles. This attachment is followed by a very slow fusion into particles having a radius of approx. 280 Å. Sonication of this mixture yields large aggregates. Electron micrographs of deoxycholate-solubilized apo B indicate an arrangement of apo B resembling strings of beads. During incubation, these particles also attach to the ternary microemulsion particles and, upon sonication, spherical particles result which resemble native LDL particles in size. Scanning chromatography corroborates the electron microscopy results. By appropriate choice of display angles in a quasi-three-dimensional display of the scanning data (corrected for gel apparent absorbance) taken at equal time intervals during passage of a sample through the column, changes in molecular radius of less than 10 Å can be detected visually. Such a display gives a quantitative estimate of 101 ± 2 Å for these particles (compared to 110 Å for native LDL). The LDL-ME particles and apo B-ME particles compete efficiently with native LDL for cellular binding and uptake. Cellular association studies indicate that both LDL- and apo B-ME particles are effective vehicles for lipid delivery into cells.

1. Introduction

Low density lipoprotein (LDL), the primary transport particle for cholesterol in the blood, has been clearly implicated in the etiology of atherosclerosis [1]. It is a microemulsion, approx. 220 Å in diameter, with a nonpolar lipid core consisting of cholesteryl ester (45 wt %) and triglyceride (3 wt %). Its surface is stabilized by a monolayer of polar phospholipids (22 wt %) and cholesterol (10 wt %) and a single protein (apolipoprotein B-100, 20 wt %) [2–4].

Apolipoprotein B (apo B) functions as the ligand for the LDL receptor of the peripheral cell surface; after binding, the LDL particles are transported into the cell [5–7]. The nonpolar lipid core undergoes a liquid crystal to liquid transition near body temperature [8–13]. The significance of this finding is evident from animal models in

* Correspondence address: Box J-245, JHMHC, Department of Biochemistry and Molecular Biology, College of Medicine, University of Florida, Gainesville, FL 32610, U.S.A.
** Present address: Department of Chemistry, Bridgewater College, Bridgewater, VA, U.S.A.
*** Present address: Department of Food Science and Human Nutrition, University of Florida, Gainesville, FL 32611, U.S.A.

which atherogenesis is strongly correlated with an ordered physical state of the core lipids. Essential to understanding the atherogenicity of LDL is the elucidation of the precise lipid-lipid and lipid-protein interactions which (i) determine the physical properties and structure of the particle, (ii) influence its receptor-mediated uptake, and (iii) direct its subsequent intracellular catabolism.

To this end, Kreiger et al. [14] have reported reconstitution of LDL and replacement of the core cholesteryl esters with equal amounts of exogenous cholesteryl ester. In addition, microemulsions of binary and ternary systems of phospholipids and neutral lipids, as protein-free models for LDL, have been prepared by sonication [15–18]. The particle diameters of these microemulsion preparations are of the same order of magnitude as that of native LDL. Recently, reassembled LDL-like particles have been prepared by several procedures involving the interaction of sodium deoxycholate (DOC)-solubilized apo B with the binary microemulsions of cholesteryl oleate (ChO) stabilized by egg yolk phosphatidylcholine (EYPC) or dimyristoylphosphatidylcholine (DMPC) [10,19]. Binary and ternary complexes of apo B with EYPC and phosphatidylcholine plus cholesterol (Ch) have also been examined and were found to differ significantly from native LDL particles [21,22].

In this communication, we report the reconstitution of an LDL-like particle by a method similar to that applied by Ginsburg et al. [19], but using a ternary microemulsion consisting of ChO, free Ch and dipalmitoylphosphatidylcholine (DPPC). Only when the incubation mixture of ternary lipid microemulsion and DOC-solubilized apo B is sonicated do the resulting particles exhibit some of the structural features of native LDL, upon examination by scanning molecular sieve chromatography and other analytical methods.

2. Experimental

2.1. Materials

All chemicals were standard reagent grade unless otherwise indicated. Sodium deoxycholate (NaDOC) was purchased from Calbiochem-Behring (La Jolla, CA) and twice recrystallized from 80% ethanol. Lipid extraction was performed with diethyl ether/methanol (3 : 1, v/v). Sepharose CL-4B and all chromatographic columns were products of Pharmacia (Uppsala, Sweden). Biogel A-1.5m, Biogel A-15m, and high molecular weight protein standards and reagents for polyacrylamide gel electrophoresis were purchased from Bio-Rad (Richmond, CA). ChO (lot no. 711-DB, Eastman Kodak, Rochester, NY), Ch (C-8253, Sigma grade 99 ± %), triolein (TO) (T7140), and DL-α-phosphatidylcholine (DPPC) (no. P-6769, Sigma, St. Louis, MO) were used without further purification. Thin-layer chromatography of ChO, Ch and DPPC on silica gel H plates was performed in 90 : 12 : 1 (v/v) petroleum ether/ diethyl ether/acetic acid; spots were detected by reaction in an I_2-saturated chamber.

2.2. Methods

2.2.1. LDL

Freshly drawn plasma was obtained from the blood bank and 1 ml of a solution containing 0.01% Na_2EDTA, 0.02% NaN_3, 0.01% Thimerosal (Sigma) and 0.002% phenylmethylsulfonyl fluoride (PMSF) (Sigma) was added per 100 ml of plasma to inhibit potential proteolytic activity. Solid KBr was used to adjust the density and LDL was obtained after two centrifugation runs in a 60 Ti rotor (Beckman Instruments) for 20 h (33 000 rpm, 105 000 × g) at 4°C at each of the 1.019 and the 1.063 g/ml density cuts to prepare the lipoprotein free of VLDL lipoprotein and HDL. The isolated LDL was further purified by gel-filtration chromatography on Sepharose 6B (Pharmacia) as described elsewhere [23].

2.2.2. Isolation of apo B-DOC complexes

A solution of LDL (~ 4 mg/ml) in pH 8.5 buffer was added to an equal volume of 20 mM DOC/0.02 M $NaHCO_3$ buffer, pH 8.5, which corresponded to a weight ratio of approx. 90 g DOC/g protein, and mixed, as previously described [24]. This solution was incubated for 24 h at 6°C after which 7.0 ml were layered onto a 2.6 × 40 cm Pharmacia C26/40 column main-

tained at 6°C containing Biogel A-1.5m (200–400 mesh, Bio-Rad, control no. 207153) equilibrated with 20 mM DOC/pH 8.5 buffer. The flow rate was held constant at 8.0 ml/h by an LKB model 10202-1 peristalic pump (LKB, Gaithersburg, MD); 2.0 ml eluant fractions were collected using a Gibson (SN, 34957) microfractionator.

Using the column buffer as a blank, the absorbance of each fraction was determined at 280 and 484 nm by an OLIS (Athens, GA) Cary 14 conversion spectrophotometer and A_{280} and A_{484} were plotted against elution volume. Those fractions constituting a peak in absorbance at either wavelength were pooled separately and concentrated approx. 5-fold by ultrafiltration using an Amicon (Lexington, MA) XM-50 filter at 4°C under nitrogen. Each peak was then dialyzed at a 1:25 (v/v) ratio against 20 mM DOC/pH 8.5 buffer at 4°C for 1 day with four buffer changes.

2.2.3. Preparation of microemulsions

Microemulsions were prepared by the modified procedure of Ginsburg et al. [17] by dispersing ChO, DL-α-DPPC and Ch at a 59.6 : 30.4 : 9.4 ratio in 0.1 M KCl, 0.01 M Tris-HCl, pH 8.0, and sonicating the mixture for 480 min under a nitrogen atmosphere as outlined in fig. 1. The temperature was maintained at 52°C, the crystal melting temperature of ChO, using a Sargent (Allied Fisher Scientific) temperature-control system. Sonication was performed using a Heat Systems sonifier (W-350 Heat Systems-Ultrasonics, Plainview, NY) equipped with a standard 0–5 inch horn at a power setting of 4 (125 W output) in the 'continuous' operating mode. After sonication, the mixture was centrifuged at 79000 × *g* for 2 h in a Beckman SW 41 rotor at 4°C. The upper 1/3 of the solution (consisting of a white precipitate) was removed and the remaining mixture was further fractionated on Sepharose CL-4B in a 2.6 × 50 cm column at 25°C and a flow rate of 20 ml/h. The column was preequilibrated and eluted with 0.1 M KCl, 0.01 M Tris-HCl, 0.025% NaN_3, 0.01% Thimerosal, 0.01% EDTA, and 0.002% PMSF.

Purity of lipids following sonication was checked by thin-layer chromatography. Lipids were extracted from aqueous solution by the method of Folch et al. [25]. 40–80 μg of lipid was

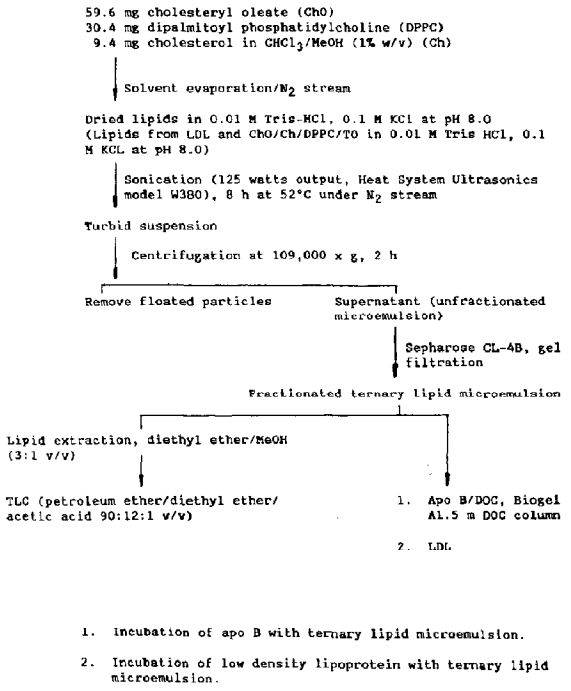

Fig. 1. Preparation of microemulsion (modified procedure of Ginsburg et al. [19]) and reconstitution experiments.

applied to TLC plates and solvent systems of chloroform/methanol/water/acetic acid (65 : 25 : 4 : 1) and petroleum ether/diethyl ether/acetic acid (70 : 30 : 2) were used to assess phospholipids (polar) and ChO and Ch (nonpolar lipids). Microemulsions were also prepared from lipid extracted from LDL was well as from quaternary lipid mixtures of ChO/Ch/DPPC/TO.

2.2.4. Reconstitution experiments

(1) Incubation of LDL with ternary lipid microemulsion (r-LDL)

2 ml of LDL ($A_{280\,nm} = 0.809$) were introduced into 1 ml of microemulsion $A_{280\,nm} = 0.420$) by an LKB perspex pump (4.8 ml/h) at room temperature. The mixture was dialyzed against 0.05 M $NaHCO_3$ buffer overnight using an S & S concentrator (Schleicher & Schuell, Keene, NH) equipped with collodion bags (UH100/10). The mixture was further incubated at 42°C for 2 h and then stored at 4°C.

(2) Incubation of apo B with ternary lipid microemulsion (r-apo B/ME)

2 ml of apo B-DOC ($A_{280\ nm} = 0.930$) were introduced to 1 ml of microemulsion ($A_{280\ nm} = 0.820$) by a perspex pump (4.8 ml/h) at room temperature. Introduction of the apo B-DOC into the incubation mixture at a more rapid rate resulted in destabilization of the emulsion. The mixture was dialyzed against 0.05 M $NaHCO_3$ buffer overnight using an S & S concentrator, UH100/10, to remove the DOC. The mixture was further incubated at 42°C for 2 h.

The incubation mixtures were further fractionated using an LKB FPLC system with a DEAE-5PW glaspore column, SN 2133-500 (LKB, Gaithersburg, MD).

2.2.5. SDS-polyacrylamide gel electrophoresis

Apo B and apo B-DOC complexes with microemulsions were electrophoresed on 5% polyacrylamide gels in the presence of 0.1% SDS, 0.1 M Tris, 0.2 M sodium acetate, and 20 mM EDTA, pH 7.4, according to the method of Weber and Osborn [26]. Reassembled apo B-microemulsion and the other samples were prepared by heating to 55°C for 1 h in the presence of 1% SDS and 1% β-mercaptoethanol in electrophoresis buffer. The gels were fixed overnight in 50% methanol/9% acetic acid and then stained with 0.125% Coomassie brilliant blue R dye in fixing solution. These gels were scanned at 590 nm using a Beckman model 24 scanning spectrophotometer and the relative mobilities of the bands on each gel determined from the corresponding peaks.

2.2.6. Chemical assays

The protein content of all samples in mg/ml was determined by the method of Lowry et al. [27], using a human serum albumin fraction V as a standard. Phospholipid content was determined by the method of Rouser et al. [28], using potassium phosphate as a standard. Samples were treated twice with 2 vols. of 2:1 $CHCl_3/CH_3OH$ so that phosphate could be detected colorimetrically at 820 nm after adding equal volumes of 2.5% ammonium molybdate and 10% ascorbic acid.

2.2.7. Electron microscopy

Electron micrographs were obtained with a Philips 301 transmission microscope, calibrated with a grating replica at a magnification of approx. × 100 000. Samples were negatively stained with 1% uranyl acetate, pH 7.4, on Formvar-coated copper grids.

2.2.8. Sedimentation velocity measurements

All sedimentation velocity runs were made on fractionated microemulsion or on incubated apo B-DOC complex with microemulsion in 0.05 M $NaHCO_3$ buffer, pH 10.0, at 42 040 rpm at 25°C in a Beckman model E analytical ultracentrifuge equipped with an RTIC unit using either a 2° wedge-sector cell or standard cell. Particle radii for equivalent spheres were calculated from the Maude-Whitmore expression [4,29–31]:

$$R_0^2 = \left[9\eta S_{w\,app}/2(\rho_p - \rho_s)\right] \quad (1)$$

using the values $\eta = 1.022 \times 10^{-3}$ g/cm per s = 0.01022 P, $\rho_s = 1.010$ g/ml, and $\rho_p = 1.045$ g/ml at 25°C, as determined by pycnometry.

2.2.9. Scanning molecular sieve chromatography (SMSC)

All SMSC experiments were performed using a direct ultraviolet-visible gel column scanning system which has been described elsewhere [23,32,33]. The basic operating routine consists of moving a 24 × 0.9 cm quartz column packed with a suitable gel (i.e., one with minimum scattering) through a horizontally collimated beam of monochromatic light at a constant rate of 0.19 cm/s for 98 s, during which transmittance is detected by an Aminco 10-267 solid-state, blank-subtract photomultiplier microphotometer through an end-on photomultiplier tube (RCA 6903 for ultraviolet or RCA C7164 for visible range).

The direct ultraviolet-visible gel column scanner system [32,33] is interfaced with a North Star Horizon Z80 microcomputer, a Sanyo DM50/2CX video display unit, and an SPG-8010 Impact Matrix printer/plotter (OLIS model 3600, Athens, GA). Gel column scans may be made at any wavelength between 220 and 1000 nm. The collection rate was approx. 10 data points per cm, which is equivalent to 192 data points for a 98 s span.

Software to display scanning data in three dimensions was written using FPZ BASIC and OLIS

graphics subroutines. This program uses a directory from files produced by the OLIS interface and allows automatic subtraction of baselines along with a routine to correct individual scans for lamp drift, if necessary. The quasi-three-dimensional display allows a choice of display angles to detect visually changes in molecular size of less than 10 Å.

2.2.10. Analysis and presentation of scanning data

The OLIS interactive software used in acquiring the data was also employed in initial stages of data analysis to create intermediate data files of two kinds:

(1) The apparent absorbance of the gel bed was removed from the data by subtracting from each sample scan a baseline scan made before introduction of the sample to the column.
(2) For comparison purposes outlined below, baseline-corrected scans made at identical times in separate experiments were added together to create 'composite scans'.

This acquisition program also provides a means for visual determination of peak positions wherein a moveable cursor is positioned at the top of a small zone and the position of the cursor along the distance axis is read from the screen. Peak positions obtained in this manner are plotted vs. the times at which scans are made, as shown in fig. 2. With the flow stopped, no corrections for finite scanning times are necessary. The value for the inverse slope is then used to calculate the partition coefficient, σ, by means of eq. 2.

$$\sigma = \frac{(dt/d\bar{x})_p - (dt/d\bar{x})_o}{(dt/d\bar{x})_i - (dt/d\bar{x})_o} \qquad (2)$$

where $(dt/d\bar{x})$ is the slope of a plot of t vs. $\bar{x}$ for a given sample marker, and the subscripts p, o and i refer to the species under investigation, the void volume marker, and the internal volume marker, respectively. Partition coefficients for molecules of known size are then used to create a calibration plot for a given gel porosity by applying the relationship developed by Ackers [34,35]:

$$a = a_0 + b_0 \mathrm{erfc}^{-1}\sigma \qquad (3)$$

where a is the hydrodynamic radius and erfc^{-1}

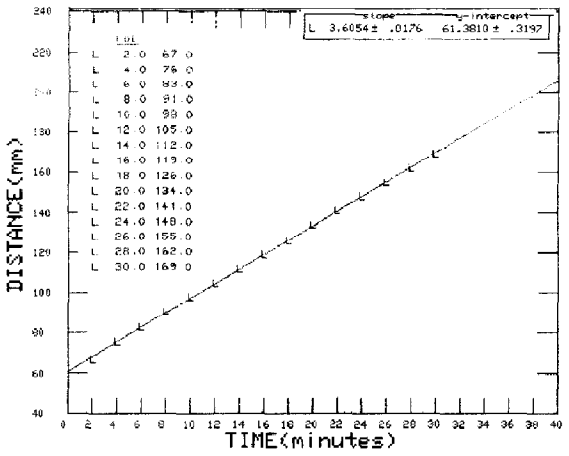

Fig. 2. Plot of distance (mm) vs. time (min) for LDL. LDL was isolated ultracentrifugally between densities 1.006 and 1.063 g/ml and passed through a 2.5×100 cm column of Sepharose Cl-4B. Samples were equilibrated with 0.05 M $NaHCO_3$ buffer, pH 10.0 and 0.05 ml of $A_{280\,nm} = 2.303$ was loaded on the top of the column. Fifteen scans were made at 2 min intervals, with the first scan at 4 min. The experiments were run on Biogel A-15m. The flow rate was 7.2 ml/h.

the inverse error function complement. Once the calibration coefficients a_0 and b_0 are determined, the partition radius of any molecule which falls within the size range of the gel porosity may be calculated by experimental determination of σ.

Since scanning times are inherently three-dimensional (in the variables distance, absorbance, and time), this laboratory has developed software to present the data in a manner which allows visualization of the three-dimensional surface which develops during passage of a sample through the column. Fig. 5 shows such a plot for a small zone of LDL (using the same series of scans from which the peak positions in fig. 5 were obtained). The program allows the user to adjust the angles of presentation (both above the time-distance plane and about the absorbance axis) to emphasize various aspects of the data. In this figure, for example, the angle about the absorbance axis has been adjusted so that the centers of the small zone peaks appear to be along the line of vision of the viewer. Such a plot also allows the experimenter to determine the homogeneity of column

packing, since deviations from linearity which would affect the determination of partition coefficients are readily apparent. Thus, one can determine immediately whether or not a column should be repacked.

2.2.11. Cell uptake studies

Normal human fibroblasts, GM5665 (Human Genetic Mutant Cell Repository, Camden, NJ), were maintained in culture and used in the 17–20th passages. Cells were seeded into 35 × 10 mm plastic dishes and grown to confluency in basal medium with Earle's salts (Gibco, Grand Island, NY) supplemented with 10% fetal bovine serum. For experiments, 24 h prior to use, growth medium was replaced with unsupplemented medium containing the growth factor, $ITSS_{\alpha}$ (Collaborative Research, Lexington, MA). Total cellular binding and uptake of LDL and modified LDL were assayed as described by Goldstein and Brown [36]. Cells were incubated in 2 ml medium containing the indicated concentrations of ^{125}I-LDL for 2 h at 37°C. For competition experiments, unlabeled LDL was added as indicated in the figure legends.

After incubation and removal of the medium, cells were washed twice with cold phosphate-buffered saline (PBS) containing 0.2% bovine serum albumin and three additional times with PBS alone. 2 ml of 0.1 M NaOH were added; the radioactivity of the hydrolysate was quantitated in a Beckman 5500 gamma counter (Palo Alto, CA). Cellular protein was determined by the method of Lowry et al. [27]. Uptake was calculated as ng ^{125}I-LDL or ^{124}I-apo B/mg cell protein. Differences between groups were tested for statistical significance by Student's *t*-test. Labeling of LDL with ^{125}I was done by the iodine monochloride technique [37].

3. Results

3.1. The Stokes radius of ternary microemulsion and of the incubation mixture with apo B

The ternary microemulsion fractionated from a Sepharose CL-4B column and then incubated with apo B was subjected to sedimentation velocity experiments (fig. 3). The Stokes radius of the incubation mixture was calculated using the Maude-Whitemore expression [29–31] and the results are shown in table 1 and fig. 2. Samples of ternary microemulsions had an average radius of 273 ± 1.3 Å, while microemulsions prepared from lipids extracted from LDL were in the range of 265 ± 1.8 Å. Microemulsions prepared from a quaternary system (CHO/DPPC/Ch/TO) had a considerably smaller radius, 245 ± 0.6 Å. Native LDL had an average radius of 110 Å.

An incubation mixture of ternary microemulsion and LDL yields particles with an average radius of 285 ± 0.5 Å. On the other hand, an incubation of ternary microemulsion with apo B-DOC complex results in particles with a radius of about 175 ± 1.0 Å. After brief sonication (60 s at 52°C and 125 W sonic energy), this mixture forms LDL-like particles. These results are consistent with the electron microscopic data.

3.2. Electrophoretic patterns of the apo B-ternary microemulsion mixtures

The electrophoretic patterns of the apo B-DOC complex isolated on a Biogel A-1.5m DOC column and the incubation mixture are shown in fig. 4. The major band at the top of the 5% acrylamide gel in fig. 4A and B represents the apo B-DOC complex, which is always predominant although some minor components are present. After incubation of apo B with the ternary microemulsion, the electrophoretic patterns show a single band (fig. 4C and D) with some residue at the top of the gel and most of the apo B sample distributed through the length of the gel.

In fig. 4C, which shows a sample incubated 2 h longer than in fig. 4D, streaking indicative of degradation is evident. Fig. 4E–G shows samples of apo B-ME complex, apo B-DOC complex, and LDL-ME complex, respectively, after 50 s sonication at 52°C and 125 W sonic energy. All three resulting patterns are distinctly similar to fig. 4A and B. Addition of microemulsion appears to stabilize the formation of apo B-ME complex. Sonication for a brief period appears to have a further stabilizing effect on all three preparations, resulting in larger aggregates. In the case of the

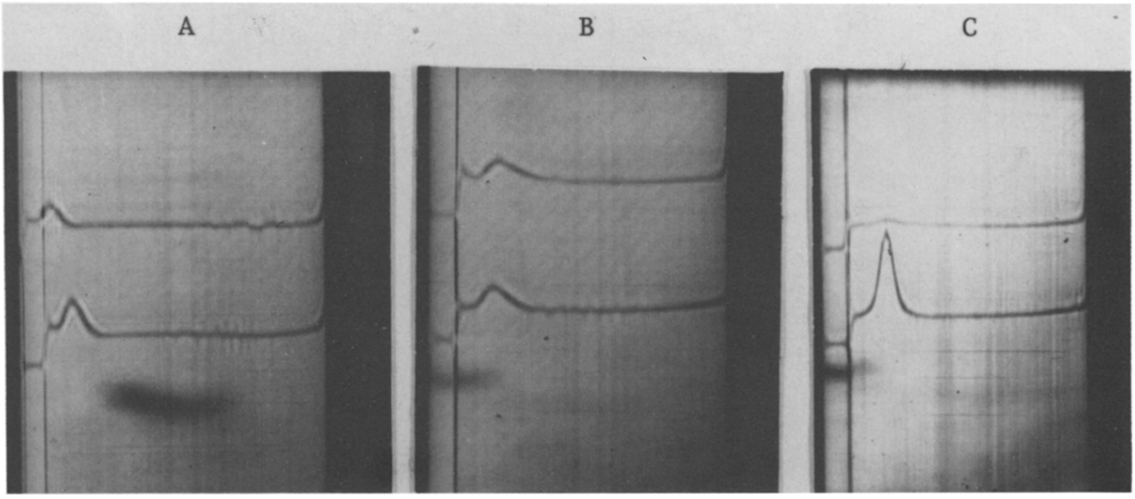

Fig. 3. Schlieren patterns of incubation mixtures of apo B with ternary lipid microemulsion. Run made at 42000 rpm. Bar angle of 60°. Incubation mixtures in 0.05 M $NaHCO_3$ buffer, pH 10.0 (A) Total elapsed time after reaching speed, 645 s. Standard cell: Sepharose CL-4B column fractionated ternary lipid microemulsion. Wedge cell: fractionated microemulsion with apo B-DOC. (B) Total elapsed time after reaching speed, 800 s. Standard cell: Sepharose Cl-4B column fractionated ternary lipid microemulsion. Wedge cell: Sepharose CL-4B column fractionated LDL lipid microemulsion. (C) Total elapsed time after reaching speed 2229 s. Standard cell: LDL, $A_{280\,nm} = 1.659$. Wedge cell: same LDL preparation as standard cell, sonicated at 125 W output sonic energy at 52°C for 1 min.

Table 1

The Stokes radii of microemulsion and of r-LDL were calculated using the Maude Whitmore expression: $R^2 = (9\eta S_{w\,app})/2(\rho_p - \rho_s)$. Average of R of microemulsion = 273 ± 1.3 Å. Average of R of LDL lipid microemulsion = 265 ± 1.8 Å.

Experiment no.	$S_{w\,app}$	R (Å)	Experimental conditions
1	12.6	169.9	Ternary microemulsion (ChO/DPPC/Ch, 60:30:10 weight ratio) and apo B-DOC complex. Incubation mixture (2:1 ratio of v/v)
2	13.3	180.0	Incubation of ternary microemulsion with apo B-DOC complex (2:1 ratio of v/v)
3	14.7	281.0	Microemulsion and LDL (2:1 ratio of v/v)
4	15.2	290.4	Microemulsion and LDL (2:1 ratio of v/v)
5	14.4	273.9	Ternary microemulsion (ChO/DPPC/Ch)
6	14.1	259.0	Ternary microemulsion (ChO/DPPC/Ch)
7	14.7	281.4	Ternary microemulsion (ChO/DPPC/Ch)
8	14.5	276.8	Ternary microemulsion (ChO/DPPC/Ch)
9	14.2	269.9	Microemulsion prepared from LDL lipid extract. Lipid extraction in $CHCl_3$/MeOH (1%, w/v)
10	14.3	263.0	Microemulsion prepared from LDL lipid extract
11	13.8	269.0	Microemulsion prepared from LDL lipid extract
12	13.7	261.0	Microemulsion prepared from LDL lipid extract
13	13.9	265.5	Microemulsion prepared from LDL lipid extract
14	12.9	245.9	Microemulsion prepared from quaternary systems (ChO/DPPC/Ch/TO)

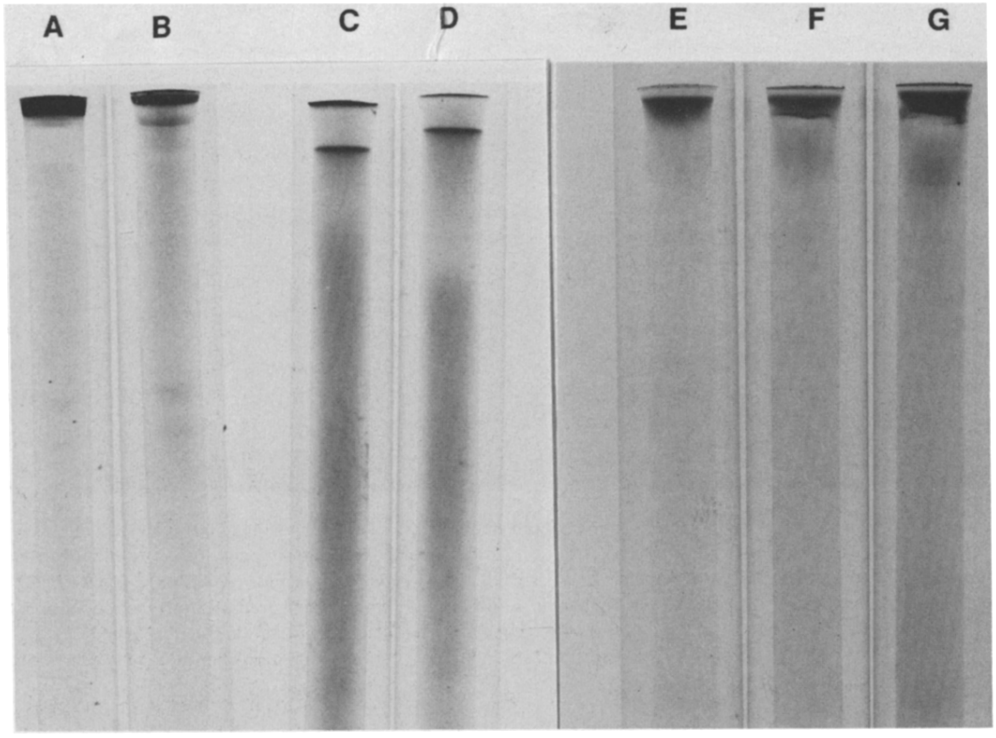

Fig. 4. SDS-polyacrylamide gel electrophoretic patterns of incubation mixtures of apo B with ternary microemulsion. (A, B) Separate preparations of apo B isolated from DOC column chromatography. Samples were prepared by heating to 55°C for 1 h; (C) apo B incubated with ternary lipid microemulsion (Sepharose CL-4B column fractionated) at 42°C for 4 h; (D) apo B incubated with ternary lipid microemulsion at 42°C for 2 h; (E) sonicated apo B-ME at pH 10.0. 1 ml of $A_{280\ nm} = 0.930$ of apo B was introduced to 2 ml of fractionated microemulsion of $A_{280\ nm} = 0.820$ by an LKB perspex pump and was dialyzed against 0.05 M $NaHCO_3$ buffer, pH 10.0, overnight using Schleicher and Schuell concentrator, S & S UH100/10. The sample was sonicated as described in section 2; (F) the same samples as (E) except that no microemulsion was added to apo B. The sample was sonicated as described in section 2; (G) incubation mixture of LDL ($A_{280\ nm} = 1.618$) with ternary lipid microemulsion ($A_{280\ nm} = 0.841$) (2:1 ratio of v/v). The sample was sonicated as described in section 2.

apo B-ME complex, sonication yields the LDL-like particles.

3.3. SMSC

Using a quasi-three-dimensional display of the scanning data taken at equal time intervals during passage of the sample through the column and by appropriate choice of display angle, it is possible to detect visually changes in molecular size of 10 Å or less, as shown in figs. 5–8D. Fig. 5 shows an LDL sample and serves as an orientation to such a quasi-three-dimensional data display. The shoulder which appears on the left of the major peak may be attributed to a slow-moving component which migrates at the same rate as the buffer and therefore serves as an internal volume marker which absorbs light at 280 nm. The shoulder on the right is a rapidly moving component consisting of aggregated species which are excluded from the gel and thus constitutes a void volume marker. Inspection of figs. 5–8D. Fig. 5 shows that in every case peaks of varying amplitude appear at the same two angles, providing a visual framework delineating the partitioning range of the gel. In figs. 5–8D, the display angle was chosen to align peaks due to the presence of any species which have the same particle radius of LDL, the

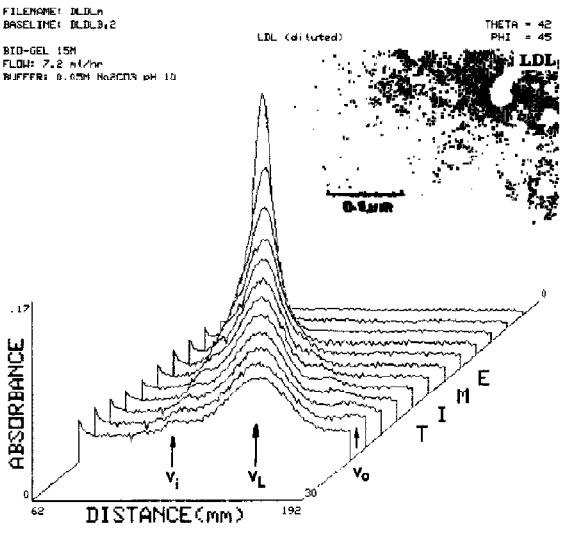

Fig. 5. Three-dimensional plot of a small zone scan of LDL preparation. LDL was isolated ultracentrifugally between densities of 1.019 and 1.063 g/ml and passed through a 2.5×100 cm column of Sepharose CL-4B. Samples were equilibrated with 0.05 M $NaHCO_3$ buffer, pH 10.0, and 0.05 ml of $A_{280\,nm} = 2.0302$ was loaded on top of the column. Absorbance vs. distance traces are plotted against the time at which scans were taken with $t = 0$ toward the rear. Scans were made at 2-min intervals on Biogel A-15m at a flow rate of 7.2 ml/h. Flow was stopped during scans. The inset shows the electron micrograph of this material.

'calibrating' of the visual display for rapid detection of such particles.

Fig. 6A–D shows the result of incubating samples of native LDL with a ternary lipid complex. Fig. 6A and B shows native LDL and the lipid microemulsion, respectively. In fig. 6C, the data from these two separate runs have been added numerically to produce the result expected if incubation of a mixed sample (at appropriate concentration) had no effect on the relative amounts of species. Comparison of this combined result with fig. 6D, where native LDL and and lipid microemulsion were incubated prior to the scanning run, shows that incubation in this case had little effect on the relative amounts of the two species and no effect at all on the size of the LDL component.

Fig. 7A–C exhibits results of various control experiments performed in order to detect the effects of a 60 s exposure to 125 W sonic energy on the various species. In fig. 7A, showing the result of such sonication of native LDL, it is obvious that there is no detectable component having the size of LDL. Sonication converts native LDL into species which are larger than the exclusion limits of this gel. Similarly, fig. 7B shows that upon sonication a sample of ternary lipid microemulsion complex remains in the form of a species which migrates at the void volume of the column. Sonication of a combined sample of native LDL and lipid gives the same result, shown in fig. 7C. It is interesting to note that a small amount of some species which is completely included into the gel can be clearly detected. Also, close inspection of fig. 7C shows a very slight indication of the presence of a species of intermediate size, but that this is very near the limits of visual detection in this type of plot.

Fig. 8A–D exhibits the results of a similar series of experiments, but substituting apo B (solubilized with DOC) for the native LDL. In fig. 8A, apo B is seen to migrate as a large (> 150 Å) aggregate in agreement with previous results [23,24]. Sonication of apo B-DOC alone has no effect on the size of this aggregate, as shown in fig. 8B. Likewise, incubation of a mixture of apo B-DOC with lipid microemulsion (fig. 8C) gives no visual indication of any interactions between these two species, since all are in the void volume region. In comparing fig. 8D with fig. 8C, however, it is obvious that treatment of an apo B-ME with a 60 s exposure to 125 W ultrasonic energy produces a new species which is visually very similar in size to native LDL, although migrating at a slightly lower rate (the line of peaks has been shifted to the left toward the internal volume marker).

Partition coefficients derived from the slopes of $\bar{x}$ vs. t plots for internal and void species along with data from standards, including native LDL, are plotted according to the method of Ackers [36] in fig. 10. Also shown in this figure is the interpolated value for the synthetic species appearing in fig. 8D. The measured value of σ for this sonicated species translates to a radius of 101 ± 2 Å, or slightly smaller than the radius of native LDL (110 Å). Since this value is outside of the range of experimental uncertainty by a factor of 4,

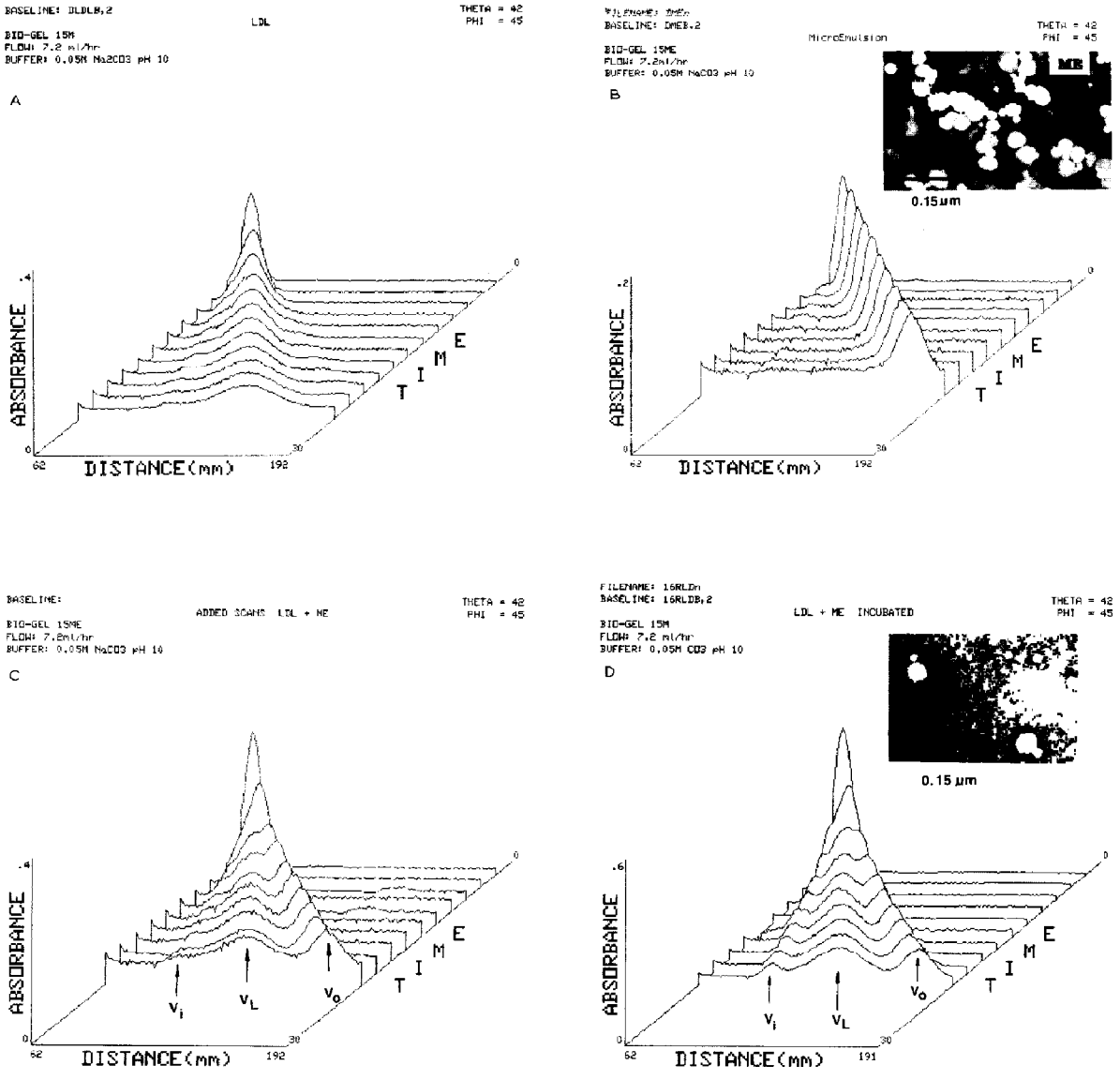

Fig. 6. (A) Three-dimensional plot of a small zone of LDL. The scanning conditions are identical to those of fig. 5 except that the absorbance at 280 nm was 1.002. (B) Three-dimensional plot of a small zone scan of fractionated microemulsions from a Sepharose CL-4B column. Ten scans were made at 2-min intervals, with the first scan taken at 4 min. The scanning experiments were run on Biogel A-15m. The flow rate was 7.2 ml/h. Samples were equilibrated and 0.05 ml of $A_{280\ nm} = 1.182$ was loaded on the top of the column. The inset shows the electron micrograph of this microemulsion. (C) Three-dimensional plot of the added scans of LDL (fig. 3A) and microemulsion (fig. 3B) in 0.05 M $NaHCO_3$ buffer, pH 10.0, on a Biogel A-15m column. Scanning conditions are identical to those of panel B. Corresponding scans of each figure were added arithmetically. (D) Three-dimensional plot of a small zone scan of a mixture of microemulsion ($A_{280\ nm} = 1.182$) and LDL samples ($A_{280\ nm} = 2.300$) (1 : 3, v/v ratio) in 0.05 M $NaHCO_3$ buffer, pH 10.0 on a Biogel A-15m column. The mixture was dialyzed against 0.05 M $NaHCO_3$ buffer overnight on an S & S concentrator, collodion bags (UH100/10). The mixture was further incubated at 42°C for 4 h. The flow rate was 7.2 ml/h. 0.06 ml of the sample mixture was loaded on the top of the column. Scans were made every 2 min. The inset shows the electron micrograph of this mixture.

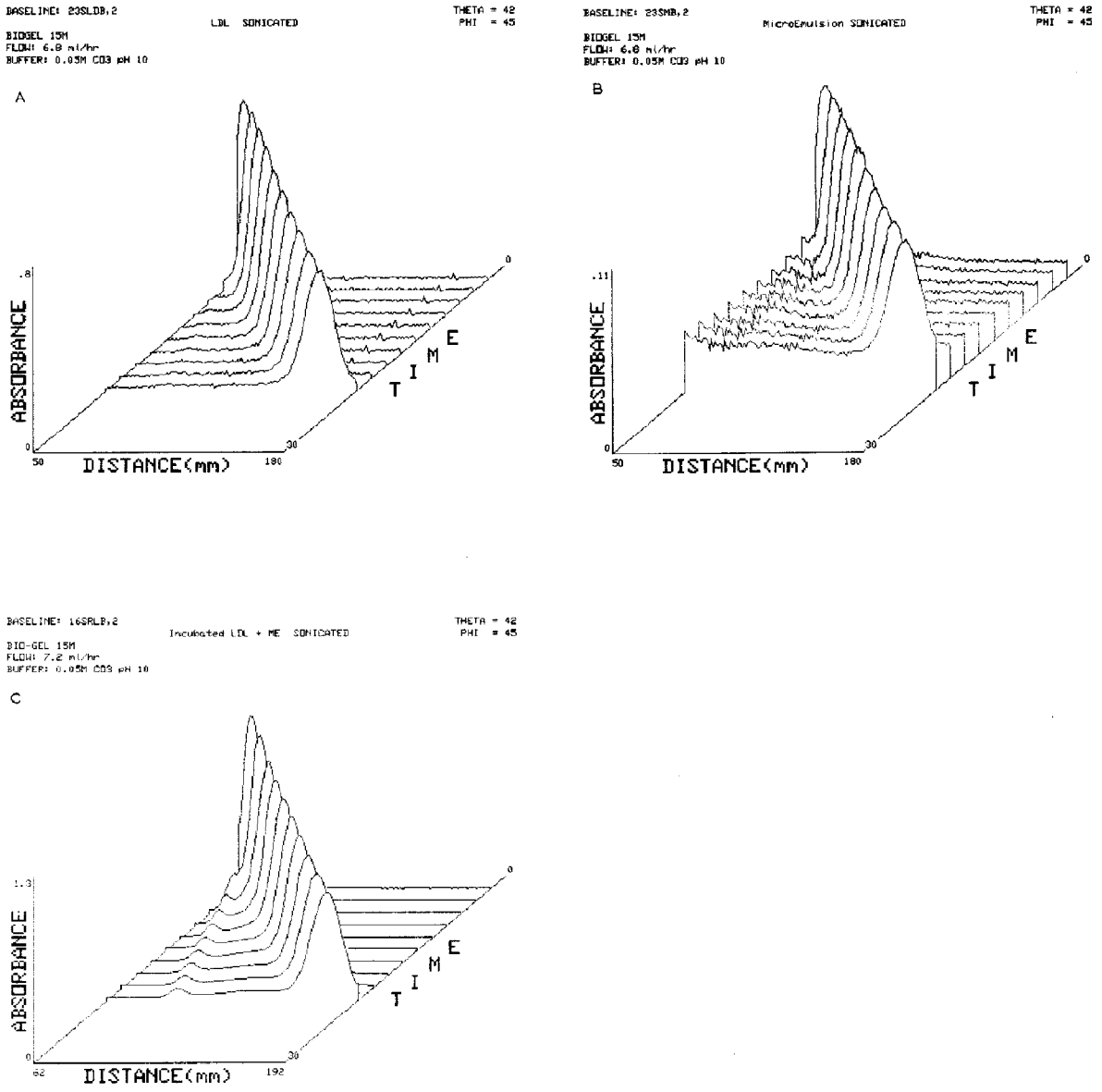

Fig. 7. (A) Three-dimensional plot of a small zone scan of sonicated LDL preparation (S-LDL). LDL samples ($A_{280\,nm} = 1.649$) were sonicated for 60 s at 52°C using a Heat Systems W-350 sonifier (125 W output of sonic energy). Ten scans were made at 2-min intervals, with the first scan taken at 4 min. The flow rate was 6.8 ml/h. Samples were equilibrated with 0.05 M $NaHCO_3$ buffer, pH 10.0, and 0.06 ml was loaded on the top of the column. (B) Three-dimensional plot of a small zone scan of sonicated microemulsion (S-ME). Sepharose CL-4B fractionated microemulsion in 0.05 M $NaHCO_3$ buffer, pH 10.0 ($A_{280\,nm} = 2.721$) was sonicated for 60 s at 52°C using a Heat Systems W-350 sonifier (125 W output of sonic energy). The scanning conditions are identical to those of fig. 6B except that the flow rate was 7.2 ml/h. (C) Three-dimensional plot of a small zone scan of mixture of microemulsion and LDL (1 : 3 ratio). LDL ($A_{280\,nm} = 2.300$) and microemulsion ($A_{280\,nm} = 1.182$) mixture was dialyzed against 0.05 M $NaHCO_3$ buffer overnight using an S & S concentrator, collodion bags UH100/10, and then the mixture was further incubated at 42°C for 4 h. The scanning conditions are identical to those of fig. 6B.

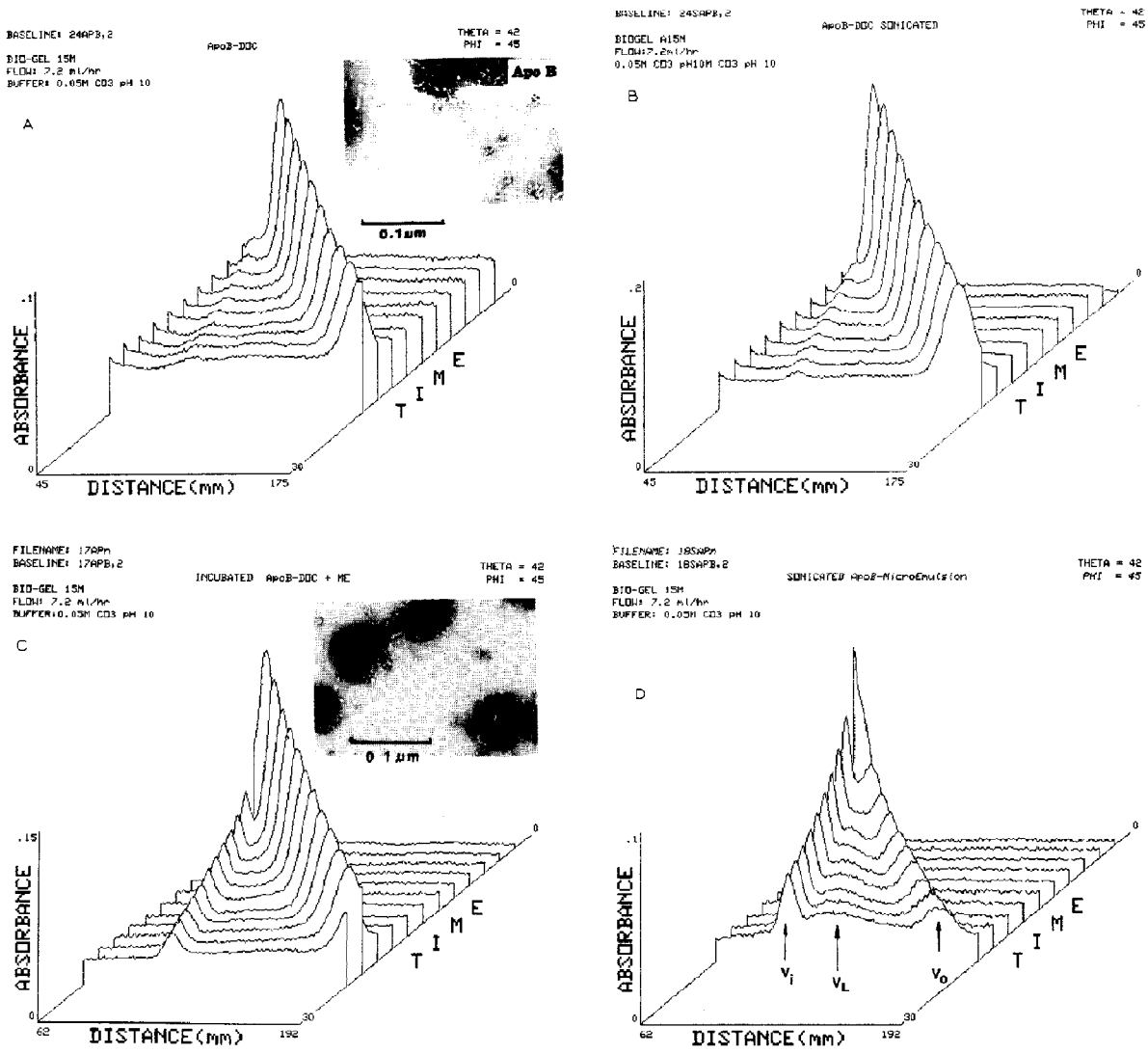

Fig. 8. (A) Three-dimensional plot of a small zone scan of apo B-NaDOC complex isolated from DOC column containing Biogel A-1.5m (Bio-Rad) (20 mM DOC in 0.2 M $NaHCO_3$ buffer, pH 8.5) (apo B-DOC). LDL samples were incubated with 20 mM DOC and dialyzed against 10 mM DOC in 0.2 M $NaHCO_3$ buffer, pH 8.5. Apo B-DOC complex ($A_{280\,nm} = 1.182$) was redialyzed against 0.05 M $NaHCO_3$ buffer, pH 10, prior to the scanning experiment. The scanning conditions are identical to those of fig. 6B. The inset shows the electron micrograph of these complexes. (B) Three-dimensional plot of a small zone scan of sonicated apo B-Na DOC. complex isolated from a DOC column containing Biogel A-1.5m (S-apo B-DOC). Samples of apo B-DOC complex ($A_{280\,nm} = 2.000$) were sonicated for 60 s at 52°C using a Heat Systems W-350 sonifier (120 W output of sonic energy). The scanning conditions are identical to those of fig. 6B. (C) Three-dimensional plot of a small zone scan of reconstituted apo B-DOC complex with Sepharose CL-4B fractionated microemulsion (r-apo B/ME). ($A_{280\,nm}$ of apo B-DOC = 2.000 and $A_{280\,nm}$ of ME = 1.182 (2 apo B : 1 ME ratio). The mixture in 0.05 M $NaHCO_3$ buffer, pH 10.0, was incubated at 42°C for 4 h. The scanning conditions are identical to those of fig. 3B. The inset shows the electron micrograph of the apo B-ME complexes. (D) Three-dimensional plot of a small zone scan of sonicated r-apo B-B complex of fig. 4C. The incubated mixture was subjected to 50 s sonication at 52°C using a Heat Systems W-350 sonifier. The scanning conditions are identical to those of fig. 3B. (The arrows indicate the appearance of r-LDL-like particles.) The incubated mixture of this figure was subjected to 60 s sonication at 52°C using a Heat Systems W-350 sonifier (125 W sonic energy). The scanning conditions were identical to those of fig. 5. Arrows indicate the void (V_0) and internal (V_i) locations as in fig. 7. Note the appearance of a species which migrates slightly more slowly than native LDL.

this difference of less than 10 Å is visually apparent upon comparing fig. 6C and 8D.

The reliability of this visual identification is borne out by examining the slopes of distance vs. time plots. Fig. 9 shows a combined plot of the results of a number of experiments of the type described above. The data clearly fall into three categories: small species migrating at the internal volume (V_i), having the lowest slopes; intermediate (LDL-sized) species; and large molecules, which are excluded from the gel beads and therefore show the largest slopes.

The results of least-squares analysis of the linear $\bar{x}$ vs. t plots have a typical uncertainty of about 1%, which via eq. 2 translates into a 4% uncertainty in calculated values for the partition coefficient, σ.

We are currently developing nonlinear least-squares curve-fitting techniques [38] which will permit determination of peak positions without operator intervention and which coupled with saturation experiments to determine point-by-point gel porosity will allow quantitative determination of the areas under the peaks, thus

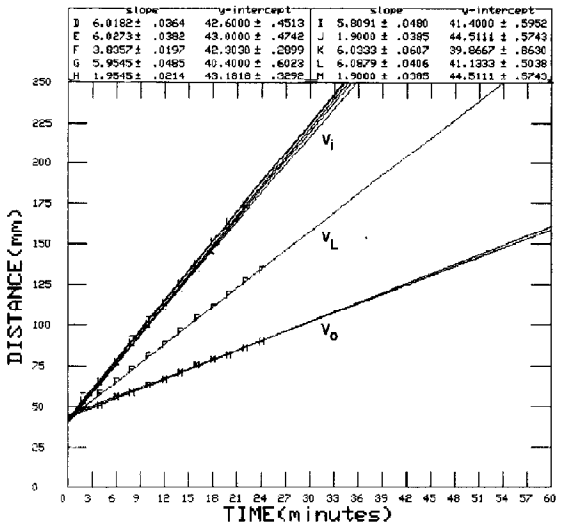

Fig. 9. Plot of distance (mm) vs. time (min) for figs. 2 and 5–8D using peak positions obtained by placing the cursor at the peak position. Uncertainties are given as the standard errors of estimate for the slope (mm/min) and y-intercept (mm) V_i = I,K,L,G,E,D; V_l = F; V_0 = H,M,J.

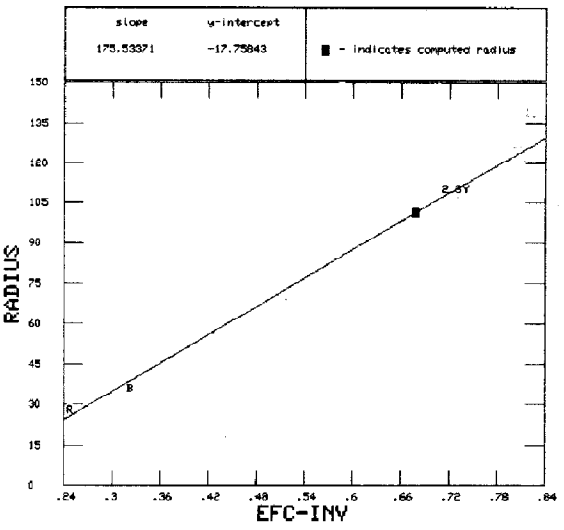

COLUMN CODE	SIGMA	EFCINV	RADIUS
B	.64880	.32204	36.00000
R	.72562	.24816	28.00000
1	.30880	.71965	110.00000
2	.31147	.71569	110.00000
3	.30063	.73192	110.00000
X	.33779	.67779	101.21602 ± 1.12247
Y	.29480	.74080	110.00000

Fig. 10. Plot of radius vs. $\text{erfc}^{-1}\ \sigma$ according to eq. 3. Partition coefficients and radii are given in table 2. The normally plotted points (1, 2, 3, Y, R, and B) are calibration molecules of known radius, while the darkened point (X) corresponds to the interpolated value for the center component (arrow indicated) of fig. 5. 1, LDL; 2, LDL; 3, LDL; Y, LDL; R, porcine rose protein; bovine serum albumin; X, unknown component (arrow indicated).

yielding detailed comparisons of relative amounts of the various separated species. Preliminary results also indicate that curve fitting to a sum of normal distributions will give information as to the extent (and possibly type) of interactions in cases where those interactions lead to skewing of small zone peaks.

3.4. Interaction between LDL or apo B-DOC complex and ternary microemulsions

Samples of LDL, apo B-DOC complex isolated by DOC column chromatography, and Sepharose

CL-4B fractionated microemulsion were chromatographed on a DEAE-5PW glaspore column, with the results shown in fig. 11. High-performance liquid chromatography shows the complex eluted at a composition of 45% ChO, 26% DPPC, 8.6% Ch and 18.3% apo B. The fractionation patterns clearly indicate that the apo B-DOC complex consists of two fractions (fig. 11B), while the microemulsion is a heterogeneous mixture containing particles of at least five or six varying sizes (fig. 11C). Fractionation of an incubation mixture of the apo B-DOC complex and ternary microemulsion at pH 8.5–10.0 resulted in a pattern which once again shows two peaks (fig. 11E), indicating that two principal components are present [23]. This reaction occurs quite rapidly at pH >8.5 and is dependent upon how quickly the NaDOC is removed from the incubation mixture. Similar fractionation of an incubation mixture of LDL and ternary microemulsion yields a highly heterogeneous population (fig. 11D), indicating either that no interaction occurs or that the rate of reaction is extremely slow throughout the pH range examined.

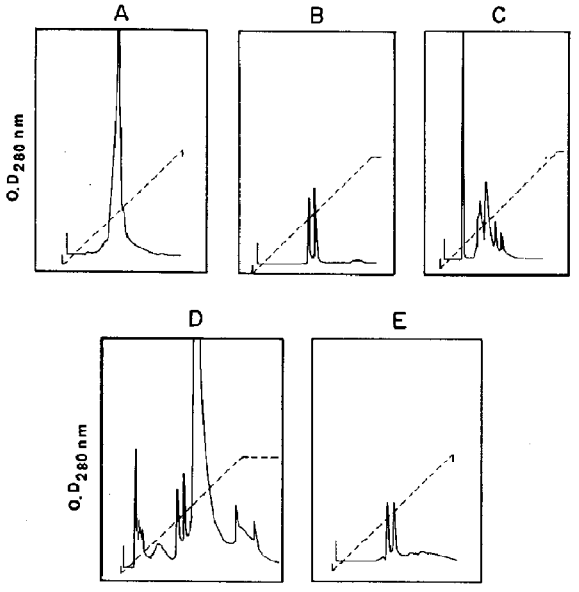

Fig. 11. Fractionation of reconstituted LDL (r-LDL, apo B-ME) using the LKB FPLC system. The DEAE-5PW glaspore column was equilibrated with 0.04 M sodium phosphate buffer, pH 7.6 in 0–1 M KCl salt gradient. (A) Human serum LDL ($A_{280\ nm}=1.396$) isolated from density of 1.060 g/ml centrifugation and followed by Sepharose 2B column fractionation. Absorbance at 0.32 full scale; (B) apo B-NaDOC complex ($A_{280\ nm}=1.067$) isolated by DOC column chromatography. Absorbance at 0.32 full scale; (C) Sepharose CL-4B column fractionated microemulsion preparation ($A_{280\ nm}=2.172$). Absorbance scale at 0.64; (D) reconstituted r-LDL. A 2:1 mixture of microemulsion ($A_{280\ nm}=2.721$) and LDL ($A_{280\ nm}=1.386$) in 0.05 M $NaHCO_3$ buffer, pH 10.0, was incubated at 42°C for 4 h; (E) reconstituted r-apo B-ME. A 2:1 ratio of apo B-DOC complex ($A_{280\ nm}=1.067$) as shown in (B) and microemulsion as shown in (C) in 0.05 M $NaHCO_3$ buffer, pH 10.0, was incubated at 42°C for 4 h. FPLC shows the complex eluted at 45% ChO, 26% DPPC, 8.6% Ch and 18.3% apo B.

3.5. Cellular uptake studies

As indicated in fig. 12, apo B-ME, LDL-ME and native LDL competed similarly with ^{125}I-LDL for binding and uptake by cultured normal fibroblasts. Fig. 13 compares the cellular uptake of ^{125}I-LDL and ^{125}I-LDL-ME; although the uptake of the LDL-ME appears to be greater, this difference is not statistically significant ($t=0.6$, 14 d.f.).

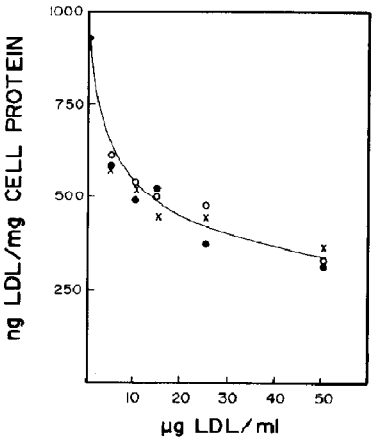

Fig. 12. Competition of unlabeled native LDL, LDL-ME and apo B-ME with ^{125}I-LDL for the cellular uptake. Normal fibroblasts were incubated for 2 h at 37°C in medium containing 10 µg ^{124}I-LDL/ml plus the indicated concentrations of unlabeled LDL (○), LDL-ME (×) or apoB-ME (○). Each point represents the mean of duplicate determinations in a representative experiment of two such experiments.

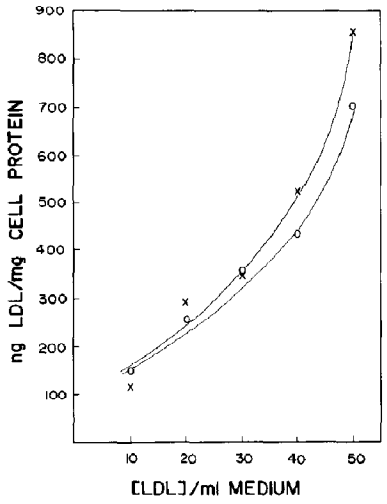

Fig. 13. Concentration-dependent cellular uptake of ^{125}I-LDL-ME compared to native ^{125}I-LDL. Normal fibroblasts were incubated for 2 h at 37°C in medium containing the indicated concentrations of native LDL or ^{125}I-LDL-ME. Total uptake values are shown. Each value is the mean of three determinations in a representative experiment of two experiments. Variations about the mean averaged 15%.

4. Discussion

Scanning gel chromatography has proven to be a useful tool in the study of reconstituted LDL-like particles. By using a gel with an appropriate porosity, the appearance of an LDL-like species is readily detected by chromatography. In addition, the scanning technique yields information which is not available from the electron microscope. A size difference of less than 10% between native LDL and the new species is visually apparent in the three-dimensional plot of fig. 8D (confirmed later by linear regression), whereas detection of a change of this magnitude is only marginally reliable in electron micrographs, given the probable distortion produced by fixation procedures. The scanning method outlined above therefore provides a more sensitive and rapid means of detecting changes in molecular species resulting from reconstitution procedures. We used this technique to provide information concerning the interaction of a stable ternary lipid microemulsion with the native LDL and with DOC-solubilized apo B, choosing the most promising cases for further examination by other methods.

Incubation of native LDL with ME results in particles with a Stokes radius slightly larger than ME alone (285 Å vs. 270 Å for ME from the ultracentrifuge results). Electron micrographs of this material (fig. 14) show what appears to be intact LDL adhering to the surface of the larger ME particles. Sonication of this complex results in a heterogeneous population of large, amorphous aggregates.

Apo B is not water-soluble upon removal from native LDL, but can be solubilized by adding surfactants such as DOC to the aqueous solvent

Table 2

Results of linear regression analysis using data from fig. 6

The inverse slopes were used to calculate σ from eq. 1 and resulting values are plotted as radius vs. $\mathrm{erfc}^{-1}\sigma$ in fig. 7 according to eq. 2. LDL samples represent four different preparations.

Species		Slope (±S.D.)	Intercept (±S.D.)	Slope^{-1}		$\mathrm{erfc}^{-1}\sigma$	Radius (Å)
Microemulsion	(0)	5.80±0.03	57.7±0.4	0.1723	(0)	–	(void)
Buffer	(I)	1.89±0.03	60.9±0.4	0.5286	(1)	–	(internal)
Porcine rose protein	(R)	2.32±0.01	58.4±0.3	0.4309	0.726	0.248	28
BSA	(B)	2.48±0.01	56.5±0.1	0.4035	0.649	0.322	36
LDL	(1)	3.54±0.08	62.7±1.1	0.2824	0.309	0.720	110
LDL	(2)	3.53±0.06	63.2±0.8	0.2833	0.312	0.716	110
LDL	(3)	3.58±0.01	58.3±0.3	0.2794	0.301	0.732	110
LDL	(Y)	3.61±0.01	61.4±0.3	0.2774	0.295	0.741	110
Unknown	(X)	3.42±0.10	56.5±1.4	0.2927	0.338	0.678	(101.2)

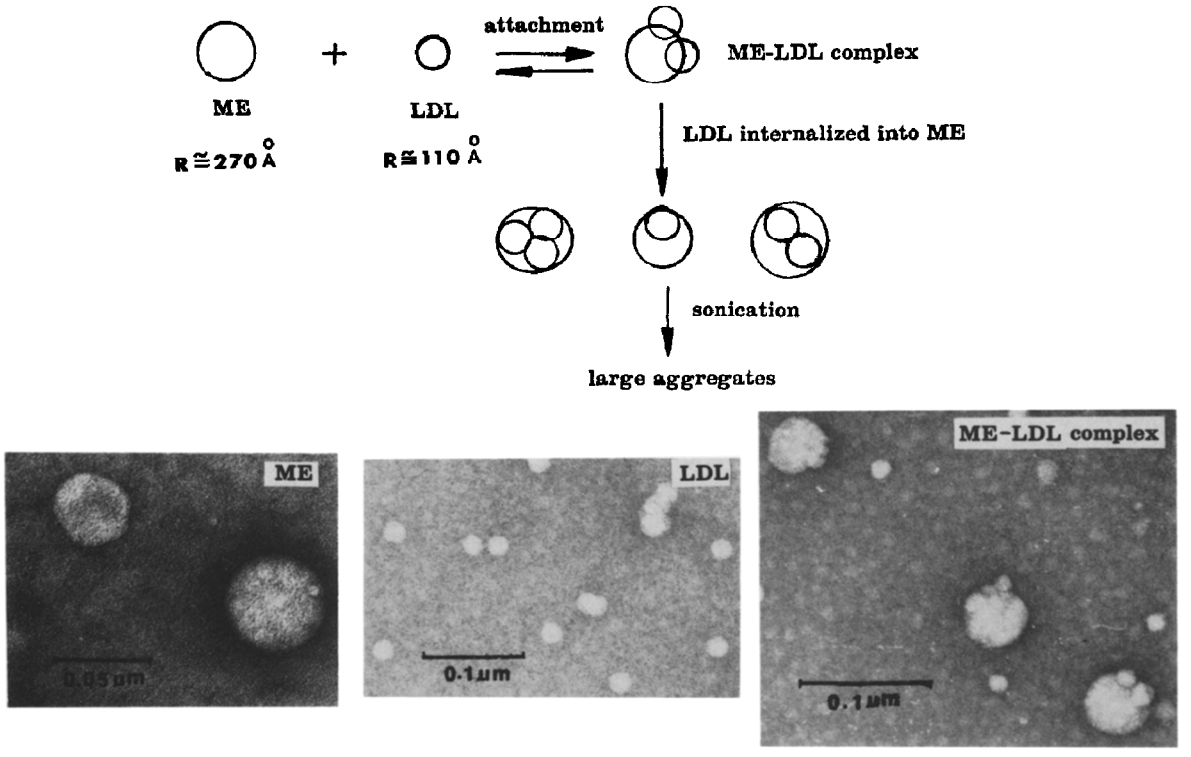

Fig. 14. A schematic representation of a plausible mechanism for the interaction of LDL and microemulsion, with electron micrographs of LDL, ME and the resulting complex.

system [23,24]. Electron micrographs of apo B-DOC show linear aggregates which appear as strings of beads. When these are incubated with ME, the strings appear to form a coating for the spherical ME particles. Upon sonication, smaller particles are found which are approximately the same size as native LDL. These smaller particles chromatograph as an independent species with a radius of 101 ± 2 Å, as compared with 110 Å for native LDL. Since LDL-like particles do not appear as a result of simple incubation of LDL/ME or of apo B-DOC/ME, it is apparent that the components of these mixtures act as stable entities, as seen in fig. 15.

Addition of certain apolipoproteins to lipid emulsions has been accomplished in vivo with the formation of a chylomicron-like particle [39]. This result, along with the above finding that sonic energy is required for formation of an LDL-like particle from apo B-ME mixtures, may indicate that a sizeable energy barrier exists which prevents spontaneous formation of LDL-like particles in vitro. Such a barrier could result from the hydrophobicity of newly synthesized apo B and the requirement that the hydrophobic domains be sequestered prior to insertion into the LDL particles. The electron micrograph and electrophoresis patterns suggest that brief sonication stabilizes the apo B-ME complex rather than disrupting it with subsequent degradation of apo B.

The competition of unlabeled LDL-ME and apo B-ME indicates that these particles are recognized and bound by the cellular LDL receptor. It has previously been reported that delipidated apo B-albumin complex competes less efficiently than native LDL for uptake [40]; the apo B-ME com-

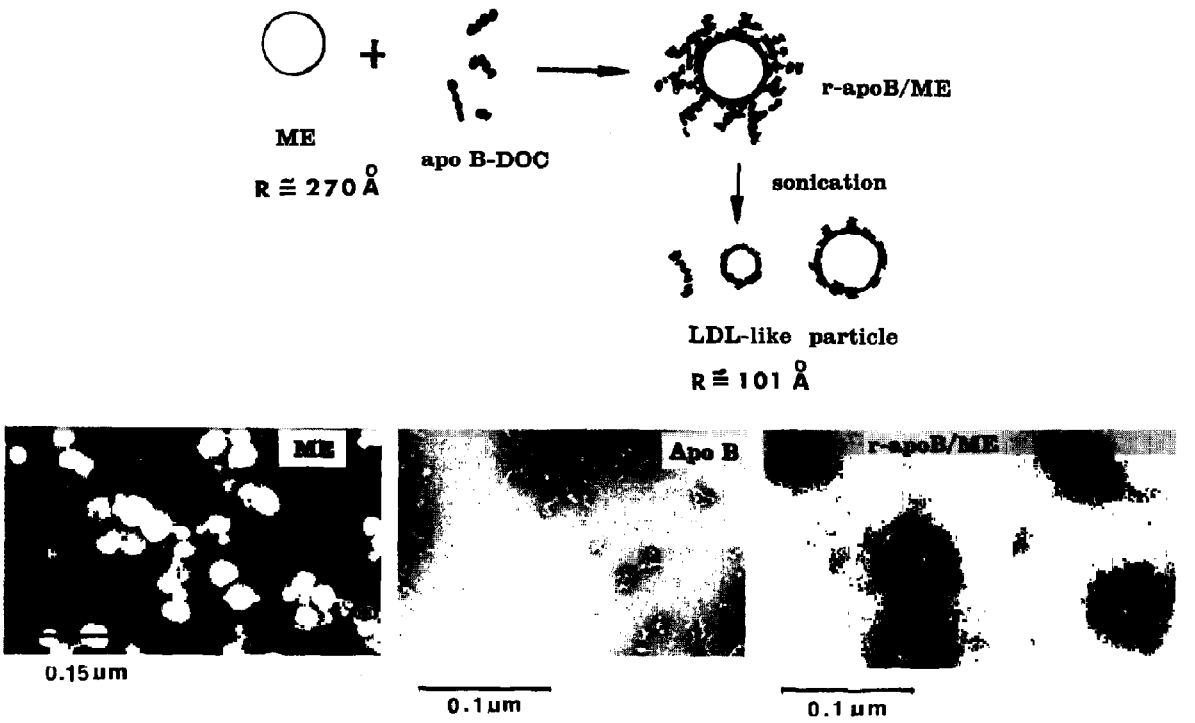

Fig. 15. A schematic representation of a plausible mechanism for the interaction of apo B-DOC complex with microemulsion to form LDL-like particles, with electron micrographs of apo B, ME and the resulting complex.

plex reported here competes very efficiently, indicating the particle resembles LDL itself. The slightly higher uptake of the labeled LDL-ME compared to native ^{125}I-LDL was somewhat surprising since previous work showed that the larger native LDL from hyperlipidemic plasma showed less cellular association than smaller LDL particles from normal plasma [41]. However, Jessup et al. [42] have shown that alteration of the charge in the lipid portion of a modified LDL influences its cell binding affinity. It is possible that the LDL-ME has a slight higher affinity for the receptor than native LDL. On the other hand, only total uptake was measured in this experiment and the possibility of greater nonspecific association cannot be ruled out. In either event, the results indicate that either apo B-ME or LDL-ME can be an effective vehicle for delivery of specific hydrophobic compounds into cells.

5. Conclusion

Based on these results, we propose two models to show the interaction between LDL or apo B-DOC complexes and the ternary microemulsions. The initial step in the interaction of LDL and microemulsion may be the attachment of the LDL to the surface of the microemulsion. In what is apparently a very slow process, the LDL molecules are engulfed by the microemulsion, forming large particles with radii of approx. 280 Å, which aggregate further upon sonication. This observation would be consistent with the data on the fusion of LDL with binary microemulsions reported by Parks et al. [43].

In the case of apo B, numerous elongated DOC-solubilized apo B molecules congregate in formations which resemble strings of beads. These apparently interact with the surface layer of the

microemulsion particles when DOC is removed. Sonication of this species results in spherical particles with partition radii of approx. 101 ± 2 Å, which closely resembles that of native LDL (110 Å).

The detection of a size difference of less than 10 Å (101 Å vs 110 Å for native LDL) demonstrates the utility of the scanning method for rapidly monitoring the results of experimental manipulations. Quasi-three-dimensional plots such as figs. 5–8D can be produced in less than 1 h after the sample is placed on the column, providing information much more rapidly than electron microscopy, ultracentrifugation, or gel electrophoresis.

This method permitted us to find a combination of experimental parameters which produces an LDL-like particle that has apparent functional similarity to LDL. The ability to assemble such particles may have important applications in delivery of hydrophobic compounds such as drugs to specific cells and in the elucidation of lipoprotein structure and metabolism, including receptor binding.

Acknowledgements

This work was supported by National Science Foundation Grant PCM 83-12101. We wish to thank Miss Donna S. Williams for her expert help with the Philips 301 transmission electron microscope studies, Ms. Inita Lillie for typing the manuscript, and Carolina Lopez for preparing the graphs.

References

1 M.S. Brown and J.L. Goldstein, Science 191 (1976) 150.
2 G.J. Nelson, in: Blood lipids and lipoproteins: Quantitative composition and metabolism (Edited by Robert E. Kreiger, New York, 1979) p. 300.
3 J. Elovson, J.C. Jacobs, V.N. Schumaker and D.L. Puppione, Biochemistry 24 (1985) 1569.
4 J.Q. Oeswein and P.W. Chun, Biophys. Chem. 14 (1981) 233.
5 R.W. Mahley and T.L. Innerarity, in: Sixth international symposium on drugs affecting lipid metabolism, eds. D. Kritchevsky, K. Paoletti and W.L. Holmes (Plenum Press, New York, 1978) p. 99.
6 T. Yamamoto, C.G. Davis, M.S. Brown, W. Schneider, M.L. Casey, J.L. Goldstein and D.W. Russel, Cell 39 (1984) 27.
7 J.L. Goldstein, R.G.W. Anderson and J.S. Brown, Nature 279 (1979) 679.
8 R.J. Deckelbaum, G.G. Shipley, D.M. Small, R.S. Lees and P.R. George, Science 190 (1975) 392.
9 R.J. Deckelbaum, G.G. Shipley and D.M. Small, J. Biol. Chem. 252 (1977) 744.
10 A.R. Tall, D.M. Small, D. Atkinson and L.L. Rudel, J. Clin. Invest. 62 (1978) 1354.
11 D. Atkinson, R.J. Deckelbaum, D.M. Small and G.G. Shipley, Proc. Natl. Acad. Sci. U.S.A. 74 (1977) 1042.
12 D. Atkinson, D.M. Small and G.G. Shipley, Ann. N.Y. Acad. Sci. 348 (1982) 284.
13 D. Atkinson, A.R. Tall, D.M. Small and R.W. Mahley, Biochemistry 17 (1978) 3930.
14 M. Kreiger, M.s. Brown, J.R. Faust and J.L. Goldstein, J. Biol. Chem. 253 (1978) 4093.
15 B. Lundburg and E.R. Saarinen, Chem. Phys. Lipids 14 (1975) 260.
16 L. Shorr, G.G. Shipley, D.M. Small and B. Sears, Biophys. J. 18 (1977) 81a.
17 G.S. Ginsburg, D.M. Small and D. Atkinson, J. Biol. Chem. 257 (1982) 8218.
18 D.P. Via, I.F. Craig, G.W. Jacobs, W.B. Van Winkle, S.C. Charlton, A.M. Gotto, Jr and L.M. Smith, J. Lipid Res. 23 (1982) 570.
19 G.S. Ginsburg, M.T. Walsh, D.M. Small and D. Atkinson, J. Biol. Chem. 259 (1984) 6667.
20 B. Lundberg and L. Saominen, J. Lipid Res. 25 (1984) 550.
21 S. Dhawan and J.A. Reynolds, Biochemistry 22 (1983) 3660.
22 R.M. Watt and J.A. Reynolds, Biochemistry 20 (1981) 2897.
23 J.Q. Oeswein and P.W. Chun, J. Biol. Chem. 258 (1983) 3645.
24 J.Q. Oeswein and P.W. Chun, Biophys. Chem. 18 (1983) 35.
25 J. Folch, M. Lees and G.H. Sloane Stanley, J. Biol. Chem. 226 (1957) 497.
26 K. Weber and M. Osborn, J. Biol. Chem. 244 (1969) 4406.
27 O.H. Lowry, N.J. Roseborough, A.L. Farr and R.J. Randall, J. Biol. Chem. 193 (1951) 265
28 G. Rouser, S. Flusher and A. Yamamoto, Lipids 5 (1970) 494.
29 A.P. Maude, and R.L. Whitmore, Br. J. Appl. Phys. 8 (1958) 447.
30 G.K. Batchelor, J. Fluid Mech. 74 (1976) 1.
31 P.W. Chun, T.E. Grow, J.Q. Oeswein and M. Fried, Fed. Proc. 39 (1980) 846.
32 E.E. Brumbaugh, E.E. Saffen and P.W. Chun, Biophys. Chem. 9 (1978) 299.
33 E.E. Saffen and P.W. Chun, Biophys. Chem. 9 (1979) 329.
34 E.E. Brumbaugh and G.K. Ackers, J. Biol. Chem. 243 (1968) 6315.
35 G.K. Ackers, Adv. Protein Chem. 24 (1970) 343.
36 J.L. Goldstein and M.S. Brown, J. Biol. Chem. 249 (1975) 5153.

37 D.W. Bilheimer, S. Eisenberg and R.I. Levy, Biochim. Biophys. Acta 260 (1972) 212.
38 E.E. Brumbaugh, M.L. Hilt, R.B. Shireman, A.J. Espinosa and P.W. Chun, Anal. Biochem. 154 (1986) 287.
39 T.G. Redgrave, Biochim. Biophys. Acta 835 (1985) 104.
40 R.B. Shireman, L.L. Kilgore and W.R., Fisher, Proc. Natl. Acad. Sci. U.S.A. 74 (1977) 5050.
41 R.B. Shireman and M.T. Coffey, J. Nutr. 114 (1984) 2373.
42 W. Jessup, G. Jurgens, J. Lang, H. Esterbauer and R.T. Dean, Biochem. J. 234 (1986) 245.
43 J.S. Parks, J.A. Martin, F.L. Johnson and L.L. Rudel, J. Biol. Chem. 260 (1985) 3155.